



Antioxidant, Antibacterial and Anti-cancer Properties of Bio-fabricated Copper-silver-zinc Nanocomposites: An Ecofriendly Approach

Madeswaran Kavipriya ^{a,b}, Dhanasekaran Selleswari ^{a*},
Unnikumar Unnimaya ^b
and Retheesh Kumar Sreedevi J. R. ^b

^a PG and Research Department of Physics, Chikkaiah Naicker College, Erode - 638004, Tamil Nadu, India.

^b Department of Physics, Hindusthan College of Arts and Science, Coimbatore- 641028, Tamil Nadu, India.

Authors' contributions

This work was carried out in collaboration among all authors. All authors read and approved the final manuscript.

Article Information

DOI: <https://doi.org/10.56557/upjoz/2024/v45i164283>

Open Peer Review History:

This journal follows the Advanced Open Peer Review policy. Identity of the Reviewers, Editor(s) and additional Reviewers, peer review comments, different versions of the manuscript, comments of the editors, etc are available here: <https://prh.mbimph.com/review-history/3816>

Original Research Article

Received: 14/05/2024
Accepted: 18/07/2024
Published: 23/07/2024

ABSTRACT

Recent advancements in nanotechnology have led to the development of bio-fabricated copper-silver-zinc nanocomposites, which exhibit multifunctional properties suitable for various applications. This study investigates their antioxidant, antibacterial, anti-cancer, and conductive properties through an eco-friendly synthesis approach. The nanocomposites were synthesized

*Corresponding author: Email: dhanasekaranselleswari@gmail.com;

Cite as: Kavipriya, Madeswaran, Dhanasekaran Selleswari, Unnikumar Unnimaya, and Retheesh Kumar Sreedevi J. R. 2024. "Antioxidant, Antibacterial and Anti-Cancer Properties of Bio-Fabricated Copper-Silver-Zinc Nanocomposites: An Ecofriendly Approach". *UTTAR PRADESH JOURNAL OF ZOOLOGY* 45 (16):15-27. <https://doi.org/10.56557/upjoz/2024/v45i164283>.

using *Allium sativum* extracts as reducing agents, ensuring minimal environmental impact and promoting sustainability. Antioxidant activities were evaluated using DPPH and ABTS, FRAP, Phosphomolybdenum and superoxide assays, demonstrating significant scavenging capabilities comparable to standard antioxidants. Antibacterial efficacy was assessed against Gram-negative bacteria, *E. coli* revealing potent inhibitory effects attributed to the synergistic action of copper, silver, and zinc nanocomposites (Cu-Ag-Zn-NC). Furthermore, the nanocomposites exhibited promising anticancer activity against breast cancer cells MCF-7, highlighting their potential as therapeutic agents. Electrical conductivity measurements confirmed their suitability for use in electronic applications, underscoring their versatility. This study underscores the eco-friendly synthesis of bio-fabricated copper-silver-zinc nanocomposites and their multifaceted properties, positioning them as promising candidates for biomedical, environmental, and technological applications.

Keywords: Antioxidants; antibacterial; anticancer; *Allium sativum*; phytochemicals.

1. INTRODUCTION

Nanotechnology has become a potential subject for creating improved materials that can be used in a wide range of fields, such as healthcare, electronics, and environmental remediation [1]. Nanoparticles are used mainly for the transmission of the therapeutic molecules (like drugs, proteins, or DNA) to the organ/ tissue of human body [2]. Copper, silver, and zinc-based nanocomposites have attracted considerable interest among the various nanomaterials due to their remarkable features, including antibacterial, antioxidant, anticancer, and conductive capacities [3]. These qualities are especially vital in tackling global concerns such as antibiotic resistance, disorders related to oxidative stress, cancer therapy, and next-generation electronic gadgets. Traditionally, the production of metal-based nanocomposites typically use chemical techniques that might potentially have negative impacts on the environment and necessitate strict procedures for disposing of hazardous waste products. On the other hand, bio-fabrication techniques that employ natural extracts or biomolecules as reducing and stabilizing agents provide a sustainable and environmentally beneficial option. This strategy not only decreases the impact on the environment but also improves the ability of the resulting nanocomposites to interact with living organisms, making them appropriate for use in medical applications [4].

The incorporation of copper, silver, and zinc in nanocomposites results in synergistic effects that enhance their individual qualities [5]. Copper ions demonstrate a wide range of antibacterial effects by breaking the cell membranes of bacteria and blocking their enzymatic activities. The antibacterial effects of silver nanoparticles are

due to their capacity to produce reactive oxygen species and attach to bacterial DNA, therefore hindering reproduction. Zinc ions, however, contribute to the systems that defend against oxidation and have a crucial function in the metabolism of cells [6]. Furthermore, the incorporation of these metals into nanocomposites improves their electrical conductivity, making them appropriate for use in sensors, actuators, and electronic devices. The conductivity of this property is essential for the advancement of innovations in wearable electronics, flexible displays, and energy storage systems [6].

This work seeks to examine the antioxidant, antibacterial, anticancer, and conductive characteristics of copper-silver-zinc nanocomposites manufactured using eco-friendly methods and derived from *Allium sativum*. This work emphasizes the promise of these nanocomposites in solving current difficulties in healthcare, environmental sustainability, and technological innovation by highlighting their multifunctionality and sustainable synthesis processes.

2. MATERIALS AND METHODS

2.1 Preparation of *Allium sativum* Extract

The leaves broth solution was made by combining 10 g of meticulously cleaned and finely ground leaves with 100 mL of sterile distilled water in a 300 mL Erlenmeyer flask. The liquid was then heated for 5 minutes and subsequently decanted for future use.

2.2 Synthesis of Nano-composites

To produce the ternary composites, precise amounts of zinc, copper, and silver salts were

combined with a 50 milliliter solution of poly (vinyl alcohol) (PVA) and distilled water. The ratios of the salts were 5% silver, 5% copper, and 90% zinc. Garlic extract was also included in the mixture. A single gram of the PVA polymer was dissolved in distilled water heated to a temperature of 80°C, resulting in the formation of the PVA-distilled water solution. The combination was continuously agitated on the hot plate-magnet stirrer for a few minutes, reducing its temperature to 50 °C. A precise amount (0.158 mol L³) of CH, NO was consistently introduced from the burette throughout the decomposition of the salt precursor. To remove the water from the dissolved mixture, the temperature of the hot plate was increased to a range of 85 to 105°C. After an additional 20 to 30 minutes, the temperature of the dry precursor fuel/surfactant gel increased to about the combustion temperature range of 153-270°C. The residual foam, resulting from combustion, was pulverized into a fine powder and subjected to calcination at a temperature of 500°C for a duration of two hours.

2.3 Characterization of Nanocomposites

The verification of the environmentally friendly production of Cu-Ag-Zn-NC was accomplished by regularly extracting samples from the reaction mixture. The absorption maxima were evaluated using a UV-vis spectrophotometer, namely the UV-3600 Shimadzu spectrophotometer, with a wavelength range of 200-800 nm and a resolution of 1 nm. Furthermore, the reaction mixture was subjected to centrifugation at a velocity of 15,000 revolutions per minute for a period of 20 minutes. The solid particles obtained were solubilized in deionized water and subsequently filtered using a Millipore filter paper having a pore diameter of 0.45 micrometers. A fraction of this filtrate, which contained a mixture of copper, silver, zinc, and nitrogen compounds, was used for scanning electron microscopy (SEM), Fourier-transform infrared spectroscopy (FTIR), X-ray diffraction (XRD) analysis, and energy-dispersive X-ray spectroscopy (EDX). A scanning electron microscope with an exceptionally high resolution, operating at a voltage of 10 kV, was employed to examine the structure and content of freeze-dried pure Cu-Ag-Zn-NC. An aliquot of 25 µl was applied onto a copper stub using a sputter coating technique for subsequent examination. The Cu-Ag-Zn-NC pictures were analyzed using an FEI QUANTA-200 scanning electron microscope (SEM). The existence of surface groups on the Cu-Ag-Zn-NC

was verified by conducting qualitative investigation utilizing FTIR spectroscopy (Stuart 2002). The spectra were obtained using a Perkin-Elmer Spectrum 2000 FTIR spectrophotometer. The EDX assays conducted by Murugan et al. [7] confirmed the presence of metals in the tested materials.

2.4 Antioxidant Properties of Cu-Ag-Zn-NC

2.4.1 DPPH antioxidant assay

The DPPH (2,2-diphenyl-1-picrylhydrazyl) assay is a widely used method to evaluate the antioxidant activity of compounds. Dissolve DPPH in an appropriate solvent (typically methanol or ethanol) to make a concentration of 0.1 mM (or 100 µM). Prepare fresh DPPH solution each time. Dissolve or dilute Cu-Ag-Zn-NC in the appropriate solvent (methanol or ethanol) to achieve desired concentrations. Typically, a range of concentrations is used to construct a dose-response curve. Add an equal volume of the DPPH solution to each well of a microplate (or cuvette if using a spectrophotometer). Use a vortex mixer or shaker to ensure uniform mixing of the DPPH solution with the test samples. Allow the reaction mixture to incubate in the dark at room temperature (or slightly below) for 30 minutes to 1 hour. The exact incubation time can vary depending on the assay conditions and the kinetics of the reaction. After incubation, measure the absorbance of each well at a wavelength of 517 nm using a microplate reader or spectrophotometer. This wavelength corresponds to the maximum absorbance of the DPPH radical.

$$\text{Inhibition (\%)} = \frac{[(\text{Absorbance of DPPH alone} - \text{Absorbance of sample}) / \text{Absorbance of DPPH alone}] \times 100}{100}$$

2.4.2 ABTS⁺ scavenging assay

Dilute the ABTS⁺ solution with water or buffer to obtain an absorbance of approximately 0.70 at 734 nm. This step may require dilution if the initial concentration of ABTS⁺ solution is too high. Dissolve or dilute Cu-Ag-Zn-NC in an appropriate solvent (such as water or methanol) to achieve desired concentrations. Prepare a range of concentrations to construct a dose-response curve. Mix equal volumes of the ABTS⁺ working solution and the test sample solutions (or solvent as a blank) in microplates or

cuvettes. Use a vortex mixer or shaker to ensure uniform mixing of the reaction mixture. Incubate the mixture in the dark at room temperature for a specific period (typically 6 minutes to 1 hour) to allow the reaction between the antioxidants and ABTS^{•+} to proceed. After incubation, measure the absorbance of each well at 734 nm using a microplate reader or spectrophotometer. This wavelength corresponds to the absorbance maximum of the ABTS^{•+} radical cation.

$$\text{Inhibition (\%)} = \left[\frac{\text{Absorbance of ABTS}^{\bullet+} \text{ alone} - \text{Absorbance of sample}}{\text{Absorbance of ABTS}^{\bullet+} \text{ alone}} \right] \times 100$$

2.4.3 FRAP antioxidant activity

Mix acetate buffer, TPTZ solution, and FeCl₃·6H₂O solution in the specified ratio (10:1:1). Prepare fresh FRAP reagent for each assay. Dissolve or dilute Cu-Ag-Zn-NC (such as water or methanol) to achieve desired concentrations. Prepare a range of concentrations to construct a dose-response curve. Mix the FRAP reagent and the test sample solutions (or solvent as a blank) in microplates or cuvettes. Use a vortex mixer or shaker to ensure uniform mixing of the reaction mixture. Incubate the mixture at a specified temperature (usually room temperature) for a defined period (typically 4 to 30 minutes) to allow the reduction of Fe(III) to Fe(II) by the antioxidants present in the samples. After incubation, measure the absorbance of each well at 593 nm using a microplate reader or spectrophotometer. This wavelength corresponds to the absorbance maximum of the colored product (ferrous tripyridyltriazine complex). Calculate the FRAP value of the samples by comparing the absorbance of the test samples with that of a standard curve prepared using known concentrations of a reference antioxidant (e.g., Trolox or ascorbic acid).

2.4.4 Superoxide radical scavenging activity

Dissolve Nitroblue Tetrazolium (NBT) in phosphate buffer to make a 1 mM solution. Prepare fresh NBT solution for each assay. Prepare a solution of NADH in phosphate buffer to make a 0.1 mM solution. This solution should also be prepared fresh for each assay. Dissolve or dilute Cu-Ag-Zn-NC in methanol to achieve desired concentrations. Prepare a range of concentrations to construct a dose-response curve. Mix equal volumes of the NBT solution, NADH solution, and the Cu-Ag-Zn-NC (or solvent

as a blank) in microplates or cuvettes. Use a vortex mixer or shaker to ensure uniform mixing of the reaction mixture. Incubate the mixture at a specified temperature (usually room temperature) for a defined period (typically 5 to 30 minutes) to allow the reduction of NBT by the superoxide radicals generated. Add an acidic solution (e.g., 1% acetic acid) to stop the reaction and stabilize the color development. After stopping the reaction, measure the absorbance of each well at 560 nm using a microplate reader or spectrophotometer. This wavelength corresponds to the absorbance maximum of the reduced formazan product formed by the reduction of NBT.

$$\text{Inhibition (\%)} = \left[\frac{\text{Absorbance of blank} - \text{Absorbance of sample}}{\text{Absorbance of blank}} \right] \times 100$$

2.4.5 Nitric acid scavenging activity

Dilute the SNP stock solution in phosphate buffer to obtain a final concentration of 10 mM. Prepare fresh SNP solution for each assay. Dissolve or dilute Cu-Ag-Zn-NC in methanol to achieve desired concentrations. Prepare a range of concentrations to construct a dose-response curve. Mix equal volumes of SNP solution and the Cu-Ag-Zn-NC (or solvent as a blank) in microplates or cuvettes. Incubate the mixture at room temperature for 30 minutes to allow for the generation of nitric oxide. After incubation, add an equal volume of Griess reagent to each well or cuvette to react with the nitrite generated from the breakdown of nitric oxide. Use a vortex mixer or shaker to ensure uniform mixing of the reaction mixture. Incubate the reaction mixture in the dark at room temperature for 10 minutes to allow color development. After incubation, measure the absorbance of each well or cuvette at 540 nm using a microplate reader or spectrophotometer. This wavelength corresponds to the absorbance maximum of the azo dye formed by the Griess reaction.

$$\text{Inhibition (\%)} = \left[\frac{\text{Absorbance of blank} - \text{Absorbance of sample}}{\text{Absorbance of blank}} \right] \times 100$$

2.4.6 Antibacterial activity of plant extract

The well diffusion method was used to test the antimicrobial activity of the Cu-Ag-Zn-NC extract against gram-negative bacterium (*E. coli*). Müller-Hinton agar (Oxoid, UK) was prepared and poured into different sterilized petri dishes, the

bacterial dilutions were prepared using the 0.5 McFarland turbidity standard and streaked separately on different agar plates. DMSO was used as negative control against the bacterial cell lines. Wells were made in the agar plates using aseptic techniques in order to add the Cu-Ag-Zn-NC. The petri dishes were then incubated at 37°C for 24 h, before measuring the zone of inhibition.

2.4.7 Anti-cancer activity

Anti-cancer activity was performed using breast cancer cell lines (MCF7). The cancer cells were cultured in DMEM media and incubated for 24 h before the treatment with the Cu-Ag-Zn-NC. 100µl of the extracts were diluted with DMSO and then added separately at four different concentrations (25 µg/ml, 50 µg/ml, 75 µg/ml, and 100 µg/ml). After the treatment, the cells were incubated for 24 hrs before assessing the effect of the different concentrations of the plant extract on the different cancer cell lines.

3. RESULTS AND DISCUSSION

3.1 Bio-physical Characterization of Cu-Ag-Zn-NC

During the UV-vis studies, we observed a significant displacement in the maximum values of the peaks. The peak absorption occurred at a wavelength of 450 nm after a duration of four hours, as shown in Fig. 1. The Cu-Ag-Zn metal

has undergone complete reduction, as evidenced by the steady increase in the surface plasmon peak of Cu-Ag-Zn- NC at 360 nm over time. After 120 minutes, the peak achieves saturation [8-10]. The variation in the concentration and size of nanoparticles may be correlated with the temporal alteration in color. Absorbance peaks can be utilized to ascertain particle size and stability. Copper-silver-zinc nanoparticles with smaller sizes exhibit a peak absorbance at approximately 360 nm, which increases as the particle size grows and decreases after the particle size surpasses the nanoscale. An XRD analysis of the Cu-Ag-Zn- NC, synthesized using garlic extract, demonstrated that its diffraction pattern corresponded to the crystal lattices (Fig. 2).

The intense peaks seen in the data matched to the (111), (110), (311), (003), (002), (001), (004), (210), and (102) Bragg reflections. These reflections can be attributed to the face-centered crystalline structure of the Cu-Ag-Zn- NC. Based on the scanning electron microscope (SEM) analysis shown in Fig. 3, the Cu-Ag-Zn-NC particles exhibited predominantly aggregation morphology and had a size range of 30 to 50 nm. The findings of our study indicate that the capped Cu-Ag-Zn- NC exhibited polydispersity and remained stable in solution for a minimum of 8 weeks. The chemical composition of the Cu-Ag-Zn- NC was revealed using the EDX pattern (Fig. 4). Evidence of the presence of pure silver, copper, zinc, and other elements confirms the

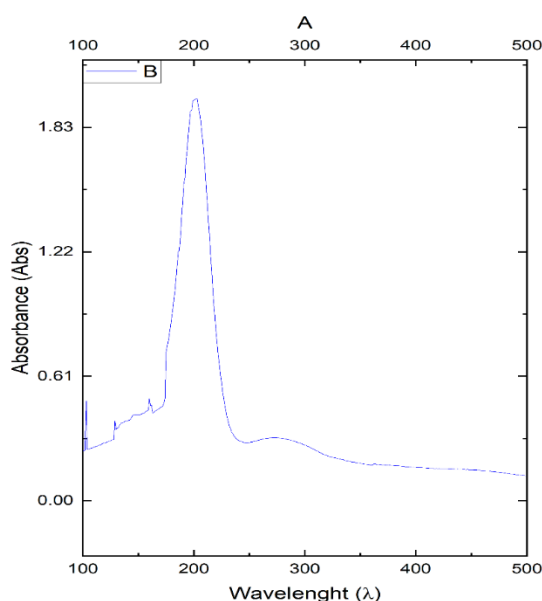


Fig. 1. UV spectroscopy analysis

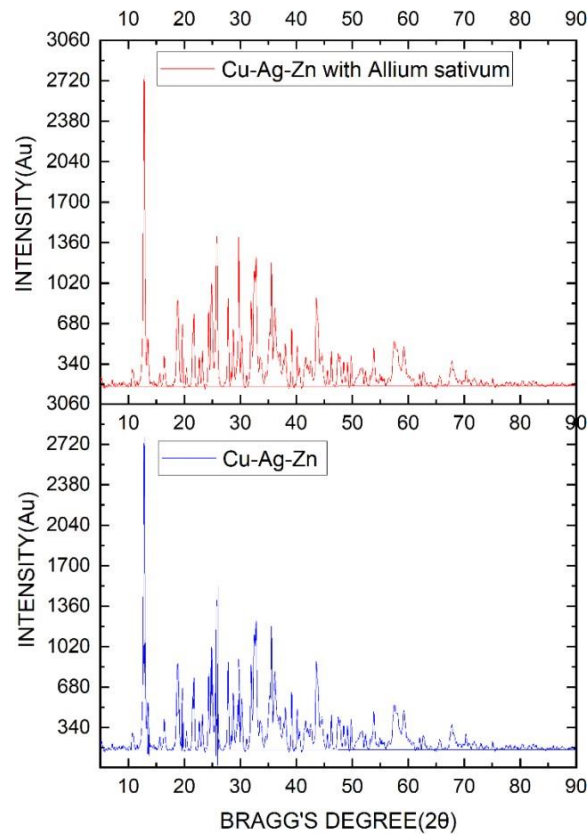


Fig. 2. XRD pattern of Cu-Ag-Zn- NC

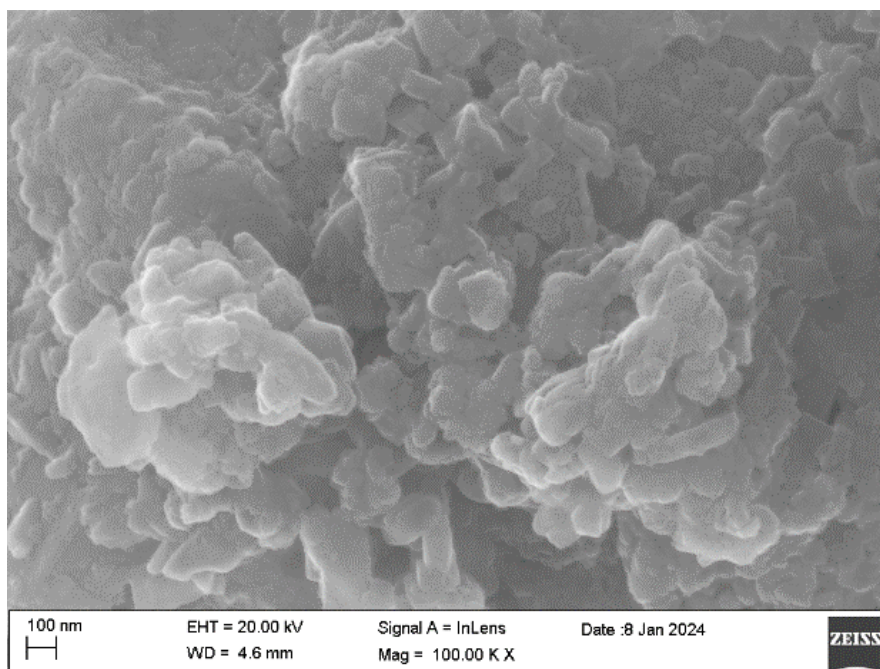


Fig. 3. SEM image of Cu-Ag-Zn- NC

biological production of Cu-Ag-Zn-NC (see to Ali et al., 2022). Furthermore, the particle size distribution of Cu-Ag-Zn-NC was determined by

dynamic light scattering, as shown in Fig. 5, and was consistent with SEM analysis. The molecule measurement dispersion indicates a size range

of around 10–80 nm, with an average particle size of 50 nm. Fig. 6 exhibits the FTIR spectrum of the water-based mixture comprising Cu-Ag-Zn- NC generated through the biosynthesis of garlic leaf extract. The notable maxima in transmittance were seen at 622, 1009, 1293, 1640, 2007, 2145, and 3374 cm⁻¹.

3.2 Antioxidant Properties of Cu-Ag-Zn-NC

3.2.1 Scavenging effects on DPPH free radical

DPPH radical quenching experiments are frequently used to assess antioxidant

capabilities. Qian et al. [11] have proven that a specific antioxidant compound effectively scavenges DPPH radicals, perhaps blocking one of the various processes by which oxidative stress is caused by lipid peroxidation. In order to assess the radical-scavenging capabilities of various concentrations of Cu-Ag-Zn- NC in our experimental setup, we found a significant and statistically significant reduction ($p < 0.05$) in the levels of DPPH as a result of the scavenging qualities exhibited by the Cu-Ag-Zn- NC (Fig. 7). The study measured inhibition percentages of 44.25%, 58.28%, 65.17%, 76.38%, and 90.96%, with rutin serving as the benchmark at 12.12%.

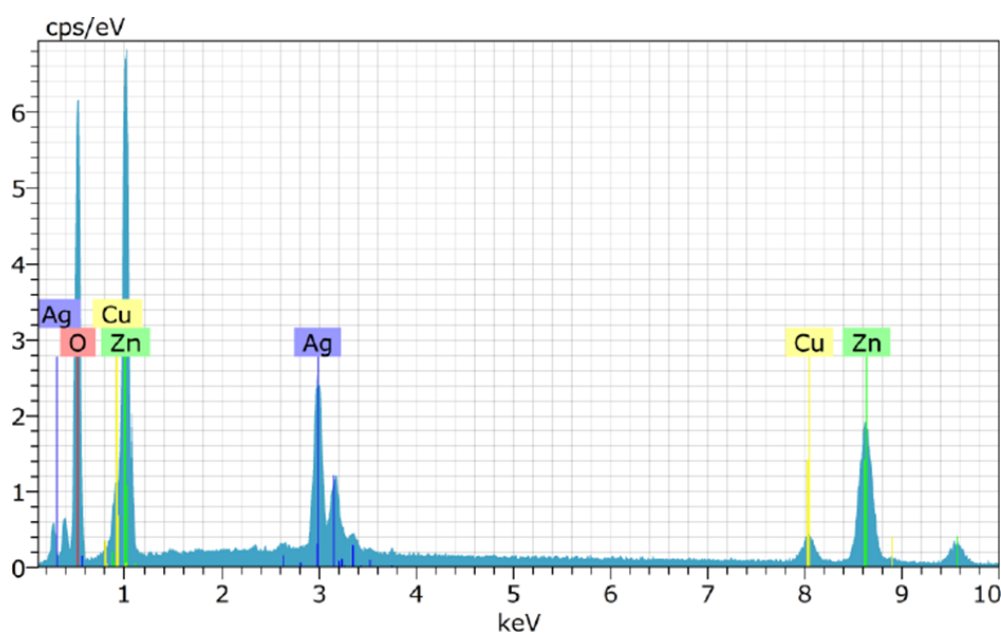


Fig. 4. EDX pattern of Cu-Ag-Zn- NC

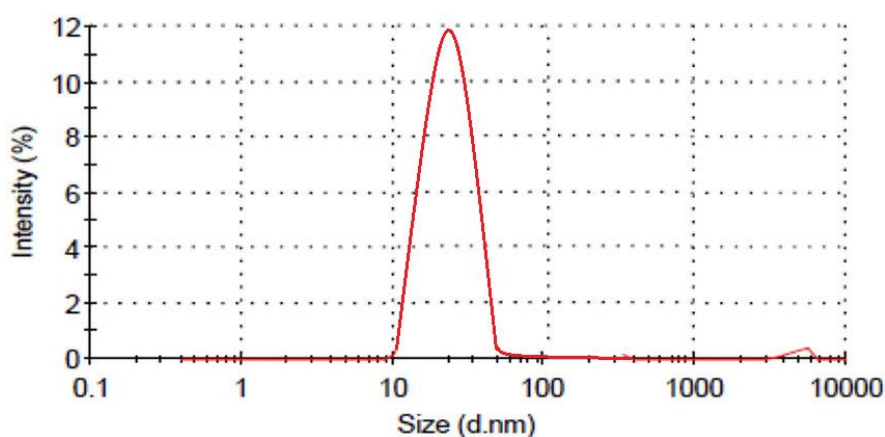


Fig. 5. DLS analysis of Cu-Ag-Zn- NC

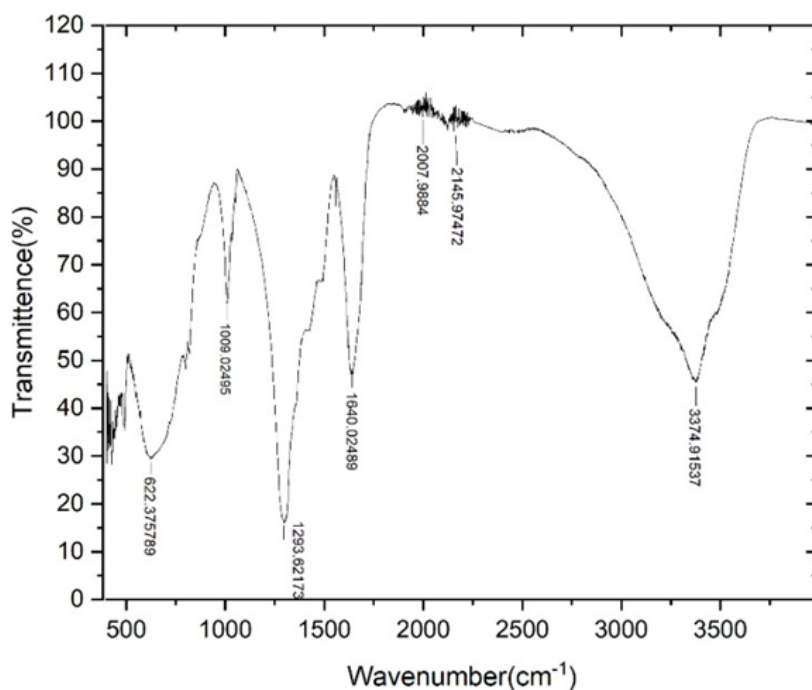


Fig. 6. FTIR spectrum of Cu-Ag-Zn- NC

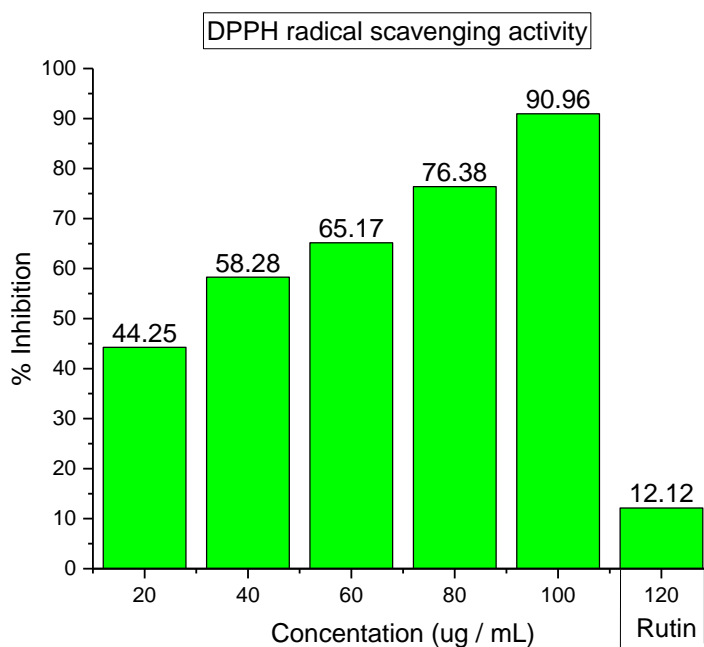


Fig. 7. DPPH free radical scavenging activity

3.2.2 Scavenging effects on ABTS free radical

Re et al. [12] demonstrated the generation of ABTS radical cation through the oxidation of ABTS using potassium persulfate. The study conducted by Shen et al. [13] found that the radical cation was reduced when exposed to

hydrogen-donating antioxidants. Ilyasov et al. [14] observed that the blue ABTS radical cation lost its hue as the chemical reaction progressed. The scavenging efficacy of different concentrations of Cu-Ag-Zn- NC on ABTS radicals showed a statistically significant increase ($p < 0.05$) as the extract concentration

increased (Fig. 8). The scavenging percentages for reducing agents vary from 33.22% to 70.18% at a trolox inhibition of 38.24%.

3.2.3 Phosphomolybdenum reduction assay

The phosphomolybdate assay is used to quantify the ability of an extract to neutralize a free radical

through electron transfer, as demonstrated in the studies conducted by Wan et al. [15] and Mamta et al. [16]. The phosphomolybdenum reduction reached its highest level of 82.44% when the concentration of Cu-Ag-Zn-NC was 100 µg/mL. The reduction percentage of standard ascorbic acid was found to be 48.87% (Fig. 9), when compared to a reference.

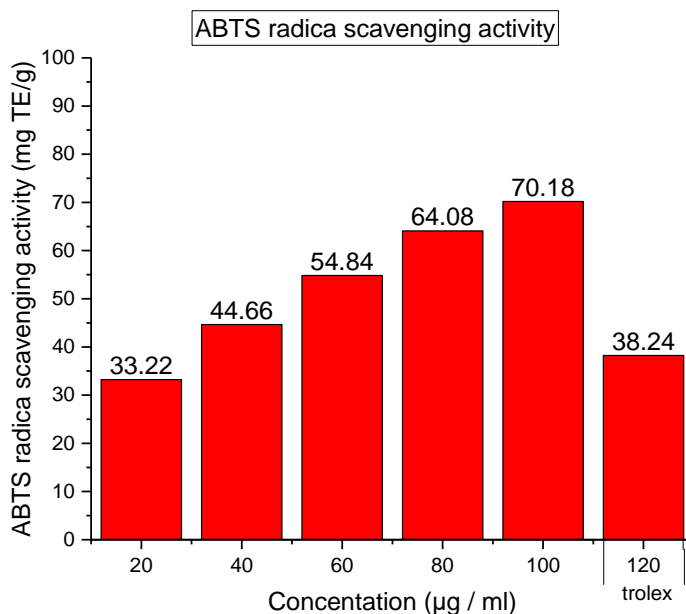


Fig. 8. ABTS free radicals scavenging activity

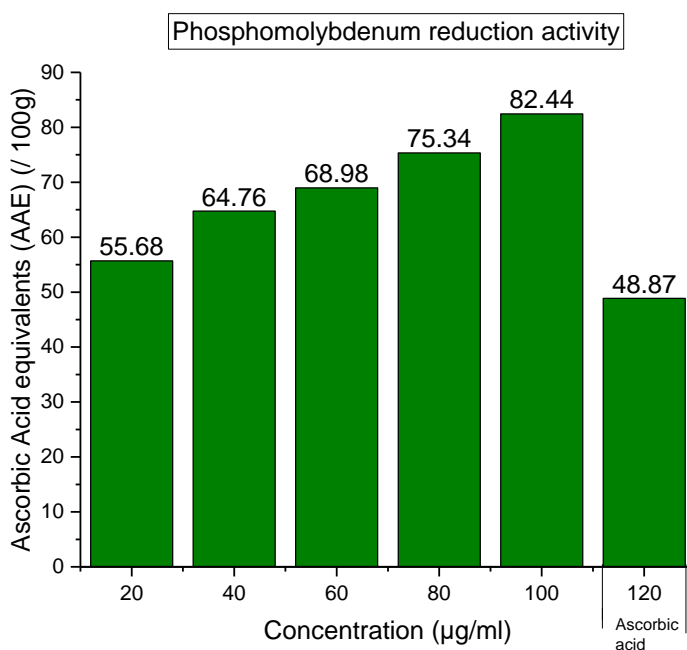


Fig. 9. Phosphomolybdenum reduction activity

3.2.4 FRAP antioxidant assay

The ferric (Fe³⁺) reducing power assay involves the conversion of Fe³⁺ to Fe²⁺ using nanocomposites derived from *A. sativum*. The aforementioned technique leads to the creation of a Ferro-ferric complex. The Cu-Ag-Zn- NC displays a variety of colors, ranging from yellow to green or blue, depending on the concentration of antioxidants present in the Cu-Ag-Zn- NC. The observed variation in color indicates the ability of the Cu-Ag-Zn- NC to successfully reduce contaminants. The ability of a molecule to undergo reduction reactions can be a reliable measure of its effectiveness as an antioxidant. The highest recorded decrease in Fe³⁺ was discovered to be 62.12% at a concentration of 100 µg/mL. In addition, it is important to mention that a decrease of 36.54% was recorded in the standard trolox at the same concentration (refer to Fig. 10).

3.2.5 Superoxide radical scavenging activity

The superoxide anion has the capacity to eliminate superoxide radicals by reducing the yellow dye (NBT²⁺) to generate blue formazan. The Cu-Ag-Zn- NC exhibited a peak superoxide radical scavenging activity of 61.23% at a concentration of 100 µg/mL. In contrast, the standard rutin demonstrated a scavenging activity of 55.87% as seen in Fig. 11. In the long term, the O₂⁻ anion has the ability to negatively

impact cellular components. The observation of a decrease in absorbance in the presence of antioxidants indicates the involvement of superoxide anion in the reaction mixture. Antioxidants have a remarkable ability to effectively prevent the production of blue nitroblue tetrazolium (NBT) precipitate. Extensive research has consistently demonstrated the efficacy of flavonoids as antioxidants, primarily due to their ability to efficiently remove superoxide anions. The findings indicate that the Cu-Ag-Zn- NC has a higher capacity to remove superoxide radicals, and its effectiveness depends on the concentration of the Cu-Ag-Zn- NC.

3.2.6 Antibacterial activity

The antibacterial effectiveness of Cu-Ag-Zn- NC against various clinically isolated strains of *Escherichia coli* germs was assessed. The experimental setup known as ZOI exhibited antibacterial effectiveness, as evidenced by the presence of a distinct region devoid of microbial growth between the wells containing the samples and a predetermined geographic distance. Conversely, water was used as a negative control to assess the impact of the solvents present in the test solution on bacterial growth. The evaluation of the zone of inhibition (ZOI) on bacterial strains was conducted after a 24-hour incubation period at a temperature of 37°C. The antibacterial effectiveness of Cu-Ag-Zn-NC was

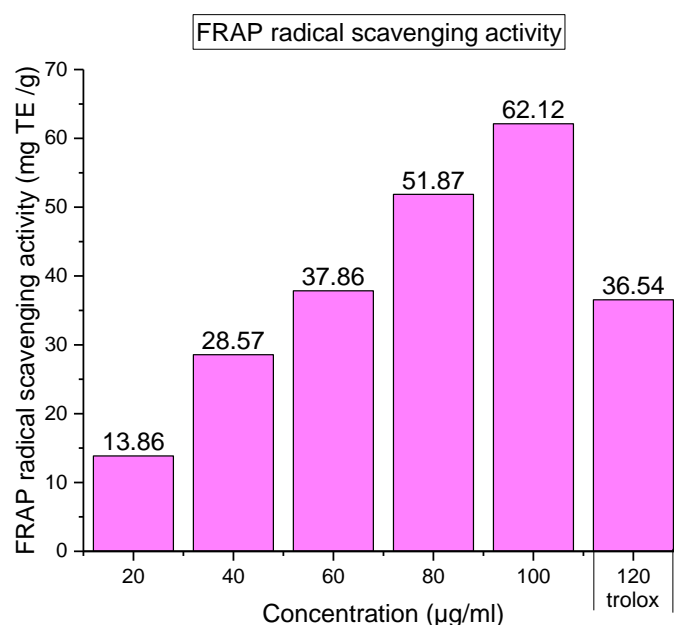


Fig. 10. FRAP scavenging activity

demonstrated against the investigated bacterial strain, as shown in Fig. 11. However, the medication was notably more effective in treating bacterial illnesses. An advantageous correlation was observed between the concentration of Cu-Ag-Zn- NC and its antibacterial efficacy. The highest concentration (500 µg/mL) exhibited the most potent antibacterial action, as indicated by the zone of inhibition (ZOI) found in Fig. 12.

3.3 Anticancer Activity

3.3.1 Cytotoxic Assay and cell viability test

The impact of Cu-Ag-Zn- NC on MCF7 breast cancer cells was assessed using the utilization of MTT assays. The cytotoxicity effects and cell survival of Cu-Ag-Zn-NC were assessed on MCF7 breast cancer cells using the MTT bioassay during a 24-hour period. The results, shown in Fig. 13, indicate that Cu-Ag-Zn-NC can

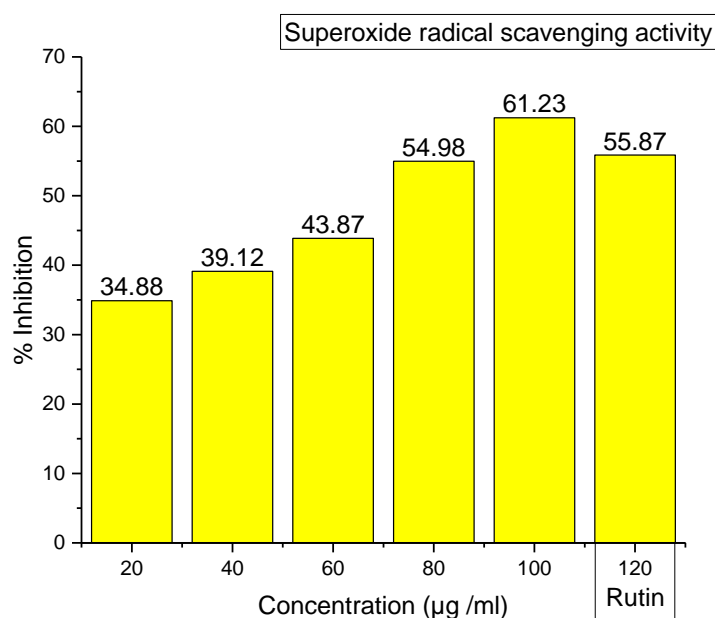


Fig. 11. Superoxide radical scavenging activity

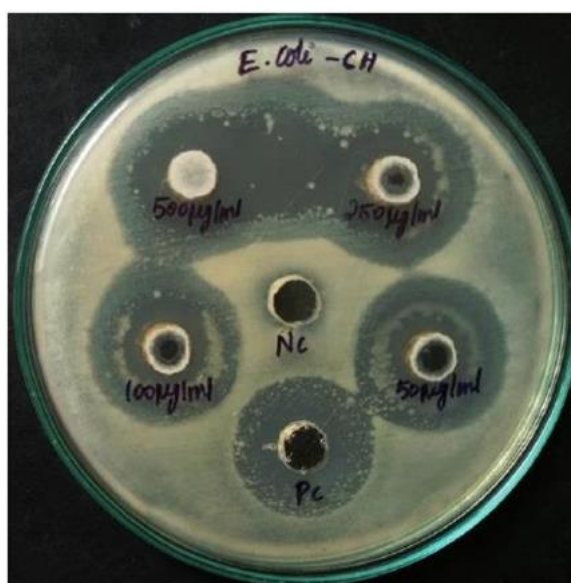


Fig. 12. Antibacterial activity of Cu-Ag-Zn- NC

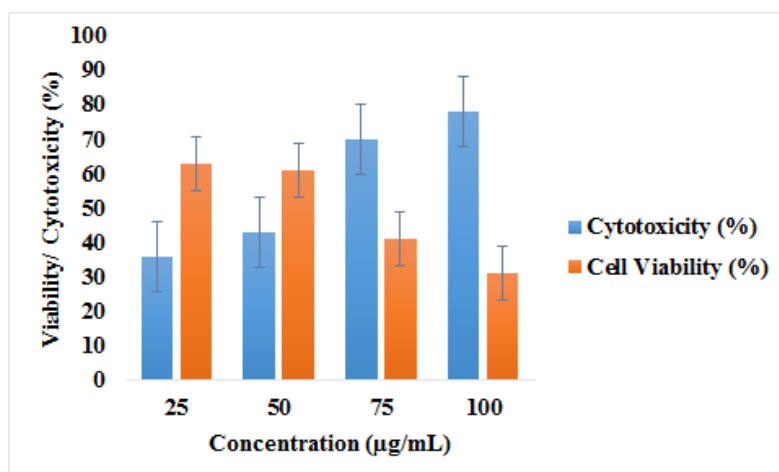


Fig. 13. Cytotoxicity and cell viability test of Cu-Ag-Zn- NC

suppress the growth of MCF7 breast cancer cells at certain concentrations (25 to 100 µg/ml). The Cu-Ag-Zn- NC exhibited cytotoxicity levels of 38%, 45%, 73%, and 88%, and cell viability levels of 66%, 63%, 42%, and 33%, respectively.

4. CONCLUSION

In conclusion, the bio-fabricated copper-silver-zinc nanocomposites demonstrate remarkable potential as multifunctional agents due to their antioxidant, antibacterial, and anti-cancer properties. The nanocomposites show promising anti-cancer effects by inducing apoptosis in cancer cells through multiple mechanisms, including oxidative stress induction and interference with cellular signaling pathways. Their selective toxicity towards cancer cells suggests potential as alternative or adjunct therapies with reduced side effects compared to conventional treatments. This eco-friendly approach offers a sustainable alternative to conventional methods, highlighting their promise in various biomedical applications. Further research is essential to fully understand their mechanisms and optimize their efficacy for practical use in healthcare and environmental sectors. Embracing these nanocomposites could pave the way for innovative solutions addressing global health challenges while promoting environmental sustainability.

DISCLAIMER (ARTIFICIAL INTELLIGENCE)

Author(s) hereby declare that NO generative AI technologies such as Large Language Models (ChatGPT, COPILOT, etc) and text-to-image generators have been used during writing or editing of manuscripts.

COMPETING INTERESTS

Authors have declared that no competing interests exist.

REFERENCES

1. Ahmed SF, Mofijur M, Rafa N, Chowdhury AT, Chowdhury S, Nahrin M, et al. Green approaches in synthesising nanomaterials for environmental nanobioremediation: Technological advancements, applications, benefits and challenges. *Environmental Research*.2022;204:111967.
2. Fattahi FS, Zamani T. Poly (lactic acid) nanoparticles: A promising hope to overcome the cancers. *Journal of Advanced Biomedical Sciences*. 2022; 11(2).
3. Unal I, Aydoğdu B, Aytar M. Plant extract-based biosynthesis of silver nanoparticle and silver-zinc nanocomposites-doped hydroxyapatite and its antimicrobial activity. *Advances in Applied Ceramics*. 2024;17436753231219539.
4. Hassan T, Salam A, Khan A, Khan SU, Khanzada H, Wasim M, et al. Functional nanocomposites and their potential applications: A review. *Journal of Polymer Research*. 2021;28(2):36.
5. Abebe B, Kefale B, Leku DT. Synthesis of copper-silver-zinc oxide nanocomposites for 4-nitrophenol reduction: Doping and heterojunction. *RSC Advances*. 2023; 13(7):4523-4529.
6. Gurgur E, Oluyamo SS, Adetuyi AO, Omotunde OI, Okoronkwo AE. Green synthesis of zinc oxide nanoparticles and

- zinc oxide–silver, zinc oxide–copper nanocomposites using *Bridelia ferruginea* as biotemplate. SN Applied Sciences. 2020;2(5):911.
7. Murugan K, Benelli G, Ayyappan S, Dinesh D, Panneerselvam C, Nicoletti M, et al. Toxicity of seaweed-synthesized silver nanoparticles against the filariasis vector *Culex quinquefasciatus* and its impact on predation efficiency of the cyclopoid crustacean *Mesocyclops longisetus*. Parasitol. Res. 2015a;114:2243-2253.
 8. Madhiyazhagan P, Murugan K, Kumar AN, Nataraj T, Dinesh D, Panneerselvam C, et al. Sargassum muticum-synthesized silver nanoparticles: An effective control tool against mosquito vectors and bacterial pathogens. Parasitol. Res. 2015;114:4305-4317.
 9. Dinesh D, Murugan K, Madhiyazhagan P, Panneerselvam C, Mahesh Kumar P, Nicoletti M, et al. Mosquitocidal and antibacterial activity of green-synthesized silver nanoparticles from Aloe vera extracts: Towards an effective tool against the malaria vector *Anopheles stephensi*?. Parasitol. Res. 2015;114:1519-1529.
 10. Narayanan M, Priya S, Natarajan D, Alahmadi TA, Alharbi SA, Krishnan R, et al. Phyto-fabrication of silver nanoparticle using leaf extracts of *Aristolochia bracteolata* Lam and their mosquito larvicidal potential. Proc. Biochem. 2022; 121:163-169.
 11. Qian H, Chen W, Sheng GD, Xu X, Liu W, Fu Z. Effects of glufosinate on antioxidant enzymes, subcellular structure, and gene expression in the unicellular green alga *Chlorella vulgaris*. Aquatic Toxicology. 2008;88(4):301-7.
 12. Re R, Pellegrini N, Proteggente A, Pannala A, Yang M, Rice-Evans C. Antioxidant activity applying an improved ABTS radical cation decolorization assay. Free Radical Biology and Medicine. 1999;26(9-10): 1231-7.
 13. Shen GB, Xie L, Wang YX, Gong TY, Wang BY, Hu YH, et al. Quantitative estimation of the hydrogen-atom-donating ability of 4-substituted hantzsch ester radical cations. ACS Omega. 2021;6(36): 23621-9.
 14. Ilyasov IR, Beloborodov VL, Selivanova IA, Terekhov RP. ABTS/PP decolorization assay of antioxidant capacity reaction pathways. International Journal of Molecular Sciences. 2020;21(3):1131.
 15. Wan C, Yu Y, Zhou S, Liu W, Tian S, Cao S. Antioxidant activity and free radical-scavenging capacity of *Gynura divaricata* leaf extracts at different temperatures. Pharmacognosy Magazine. 2011;7(25):40.
 16. Mamta, et al. Antioxidants, in Biotransformation of Waste Biomass into High Value Biochemicals, S.K. Brar, G.S. Dhillon, and C.R. Soccol, Editors. 2014, Springer New York: New York, NY. 2014; 117–38.

Disclaimer/Publisher's Note: The statements, opinions and data contained in all publications are solely those of the individual author(s) and contributor(s) and not of the publisher and/or the editor(s). This publisher and/or the editor(s) disclaim responsibility for any injury to people or property resulting from any ideas, methods, instructions or products referred to in the content.

© Copyright (2024): Author(s). The licensee is the journal publisher. This is an Open Access article distributed under the terms of the Creative Commons Attribution License (<http://creativecommons.org/licenses/by/4.0>), which permits unrestricted use, distribution, and reproduction in any medium, provided the original work is properly cited.

Peer-review history:

The peer review history for this paper can be accessed here:

<https://prh.mbimph.com/review-history/3816>